J Mater Sci: Mater Electron (2017) 28:14678–14684
DOI 10.1007/s10854-017-7333-4

Nano-sized CuO/ZnO hollow spheres: synthesis, characterization and photocatalytic performance

Mohammad Hassanpour[1] · Hossein Safardoust-Hojaghan[1] · Masoud Salavati-Niasari[1] · Ali Yeganeh-Faal[2]

Received: 11 May 2017 / Accepted: 8 June 2017 / Published online: 12 June 2017

Abstract CuO/ZnO hallow spherical nanocomposite were synthesis with rapid microwave method in polyol solvent at 10 min and 900 W as optimum time and power. Prepared CuO/ZnO is characterized by X-ray diffraction analysis, Fourier transform infrared spectroscopy, scanning electron microscopy and for an estimate the band gap used diffuse reflectance measurement. For the sufficient optical properties, prepared CuO/ZnO nanocomposites are applied as a catalyst in photodegradation of rhodamine B (RB) and methylene blue (MB) pollutants. Results showed that after 120 min, 41 and 73% of RB and MB was degraded respectively.

1 Introduction

In recent years, the rapid development of industry improves the quality of people's living standards and at the same time also causes serious environmental problems, especially water pollution [1, 2]. Water pollution can be created with entering toxic substance into water bodies such as lakes, rivers, oceans and so on, getting dissolved in them, lying suspended in the water or depositing on the bed, so decreases quality of water [3, 4]. Organic contaminants are the most important pollutant that can produce from sources such as textile, paint, paper and plastic industries [5]. The commonly used methods for handling these organic pollutants are filtration, oxidation and adsorption, but they cannot containment organic pollutants completely [6–8]. Nanotechnology can play key role in solving water problems related to quality and quantity [9–12]. Among nanotechnology based process for removing organic pollutants, photocatalyst process is an efficient, economical and environmentally friendly technology. In this process, oxidation of organic pollutants is accelerated by the presence of a catalyst [13–16]. Nanocomposites can act as suitable photocatalytic agent. ZnO based nanocomposites are very interesting for photocatalytic degradation for its advantages such as direct band gap, anisotropic growth, high electron mobility and simple controlling of its morphology [17, 18]. On the other hand, CuO nanostructures for their unique properties have been found many applications in catalyst, sensor and ceramic fields [19, 20].

Till now, many studies have been assigned to investigate ZnO and CuO nanostructures separately, but there are limited research on investigation of CuO/ZnO nanocomposite. Karuthapandian and co-workers have synthesized CuO/ZnO nanorods by simple chemical method. They investigated photocatalytic activity of nanocomposite against mixed dye solutions [21]. Prabhu et al. have prepared p-CuO/n-ZnO heterojunction film. They have examined the influence of annealing temperature on the physical properties of CuO and ZnO thin films [22]. CuO/ZnO nanocomposites have been synthesized by hydrothermal method by Wu and co-workers. They investigated magnetic properties of prepared nanocomposites [23].

Above mentioned synthesis procedures suffer from long reaction time, high temperature process and complexity. In this study, the first step, CuO/ZnO nanocomposite is synthesized via microwave method as green, simple and fast method. Prepared nanocomposite is characterized with X-ray diffraction pattern analysis, scanning electron

✉ Masoud Salavati-Niasari
Salavati@kashanu.ac.ir

[1] Institute of Nano Science and Nano Technology, University of Kashan, P.O. Box 87317-51167, Kashan, Iran

[2] Department of Chemistry, Faculty of Science, Payame Noor University, Tehran, Iran

Table 1 Different conditions of synthesis procedure

Number	Mole ratio M1:M2:S	Power (W)	Time (min)
1	1:1:220	900	5
2	1:1:220	900	10
3	1:1:220	900	15
4	1:1:390	900	10
5	1:1:220	750	10
6	1:1:220	900	10
7	1:1:220	900	Cyclic irradiation

microscopy, Fourier infrared spectroscopy and energy dispersive spectroscopy. Finally, CuO/ZnO nanocomposite is used to accelerate oxidation of MB and RB in contaminated water under UV light in photocatalytic process.

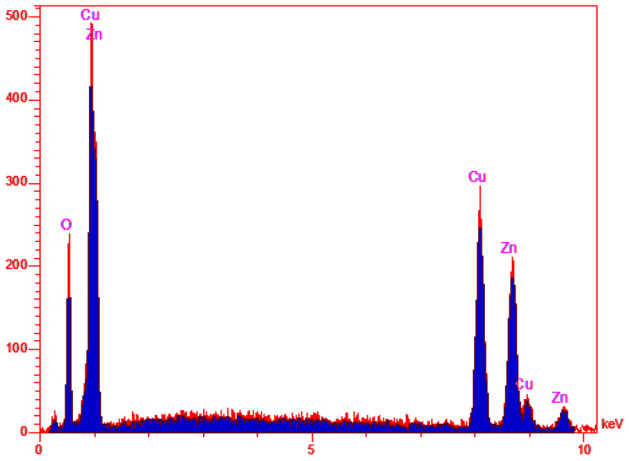

Fig. 2 EDS analysis of prepared CuO/ZnO nanocomposites in 10 min, 900 W

2 Experimental

2.1 Materials and methods

Ethylene glycol, $Cu(CH_3CO_2)_2{\cdot}4H_2O$ and $Zn(CH_3CO_2)_2{\cdot}2H_2O$ were purchased from Merck and all the chemicals were used as received without further purifications. GC-2550TG (Teif Gostar Faraz Company, Iran) were used for all chemical analyses. XRD patterns were recorded by a Philips, X-ray diffractometer using Ni-filtered CuKα radiation. SEM images were obtained using a LEO instrument model 1455VP. Prior to taking images, the samples were coated with a very thin layer of Pt (using a BAL-TEC SCD 005 sputter coater) to make the sample surface conductor and prevent charge accumulation, and obtaining a better contrast.

2.2 Preparation of [bis(salicylaldehydato)Zn(II)] and [bis(salicylaldehydato)Cu(II)]

4 mmole of acetate precursor were dissolved in 20 ml methanol under magnetic stirrer. 8 mmole of salicylaldehyde were dissolved in 20 ml methanol after that the solution was added drop wise to the metal solution and dry at room temperature.

2.3 Synthesis of CuO/ZnO nanoparticles

0.1 g of $Cu(CH_3CO_2)_2{\cdot}4H_2O$ and 0.1 g $Zn(CH_3CO_2)_2{\cdot}2H_2O$ and 6 ml ethylene glycol were stirred for 10 min. Obtained

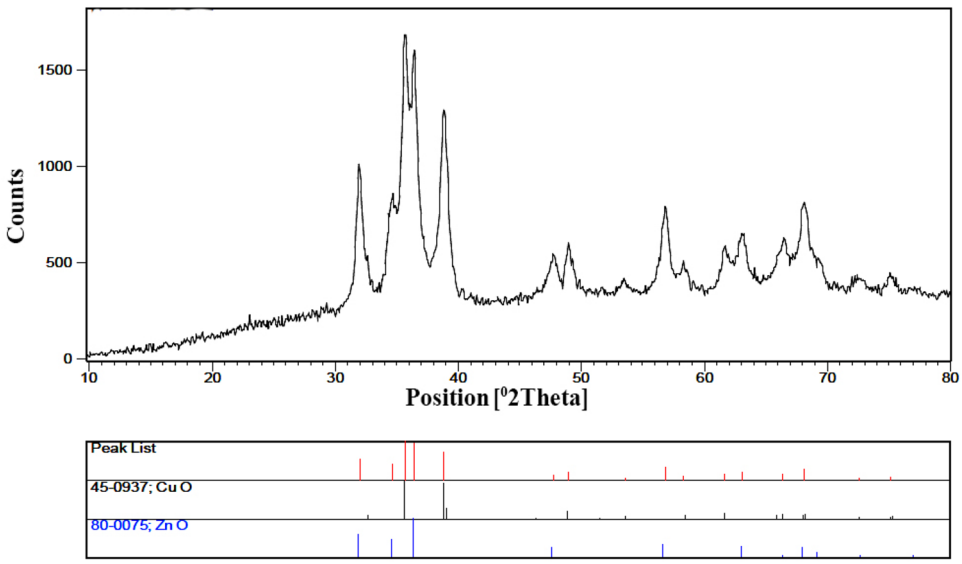

Fig. 1 XRD pattern of prepared CuO/ZnO nanocomposites in 10 min, 900 W

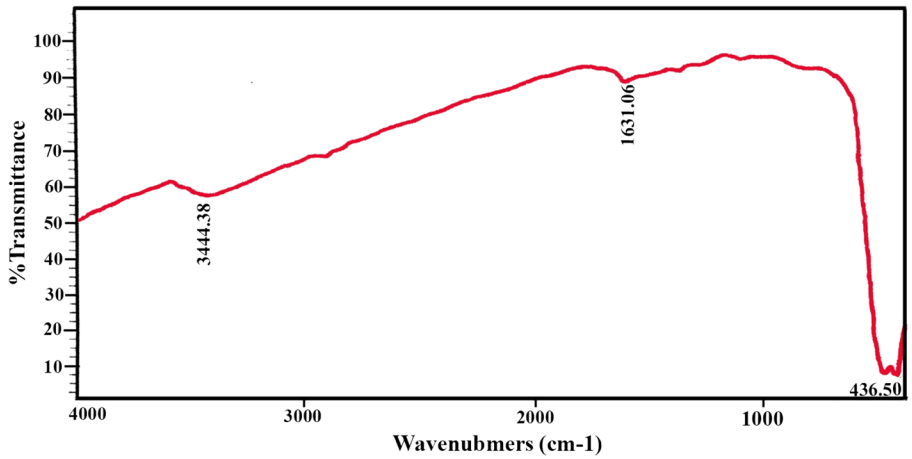

Fig. 3 FT-IR spectra of prepared CuO/ZnO nanocomposites in 10 min, 900 W

solution was put in microwave oven under irradiation. Different conditions listed in Table1 were applied. Gained precipitate was centrifuged and rinsed with distilled water. The obtained sediment was left to dry at 60 °C. For preparation of CuO/ZnO the product was calcined at 400 °C for 2 h.

2.4 Photocatalytic test

Photocatalytic activity of CuO/ZnO nanocomposite was carried out by monitoring the degradation of methylene blue and rhodamine B in aqueous solution, under irradiation with UV light. Degradation process was performed in a quartz photocatalytic reactor. Photocatalytic degradation was carried out with 10 ppm solution of dyes and 0.01 g of nanocomposite. Then the mixture was placed in photoreactor under UV light and stirred for 30 min at dark to ensure proper adsorption–desorption equilibrium of the dye molecules on the nanostructures surface required to act as an efficient photocatalyst. To maintain the solution oxygen-saturated throughout the reaction, air was blown into the vessel via a pump. Then CuO/ZnO was separated from the 5 cc samples, taken from the degraded solution at various time intervals, using 5 min centrifuging at 12,000 rpm. The dye concentration was determined with aid of a UV–Vis spectrophotometer.

3 Results and discussion

The XRD pattern of CuO/ZnO nanocomposite is shown in Fig. 1. It can be seen that prepared nanocomposites have a pure monoclinic CuO (JCPDS card No. 45-0937) and ZnO hexagonal structure (JCPDS card No. 80-0075). There are only two crystalline phase related to CuO and ZnO and no other phase related to impurity. crystalline sizes is calculated from Scherrer equation, $Dc = K\lambda/\beta Cos\theta$ [24], where

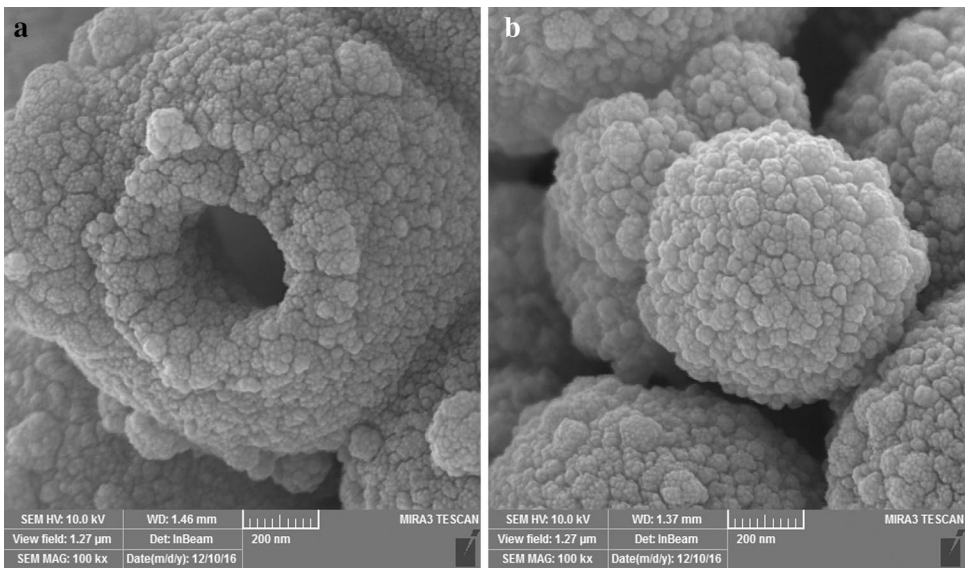

Fig. 4 SEM images of CuO/ZnO nanocomposites at **a** cyclic, **b** continuous modes

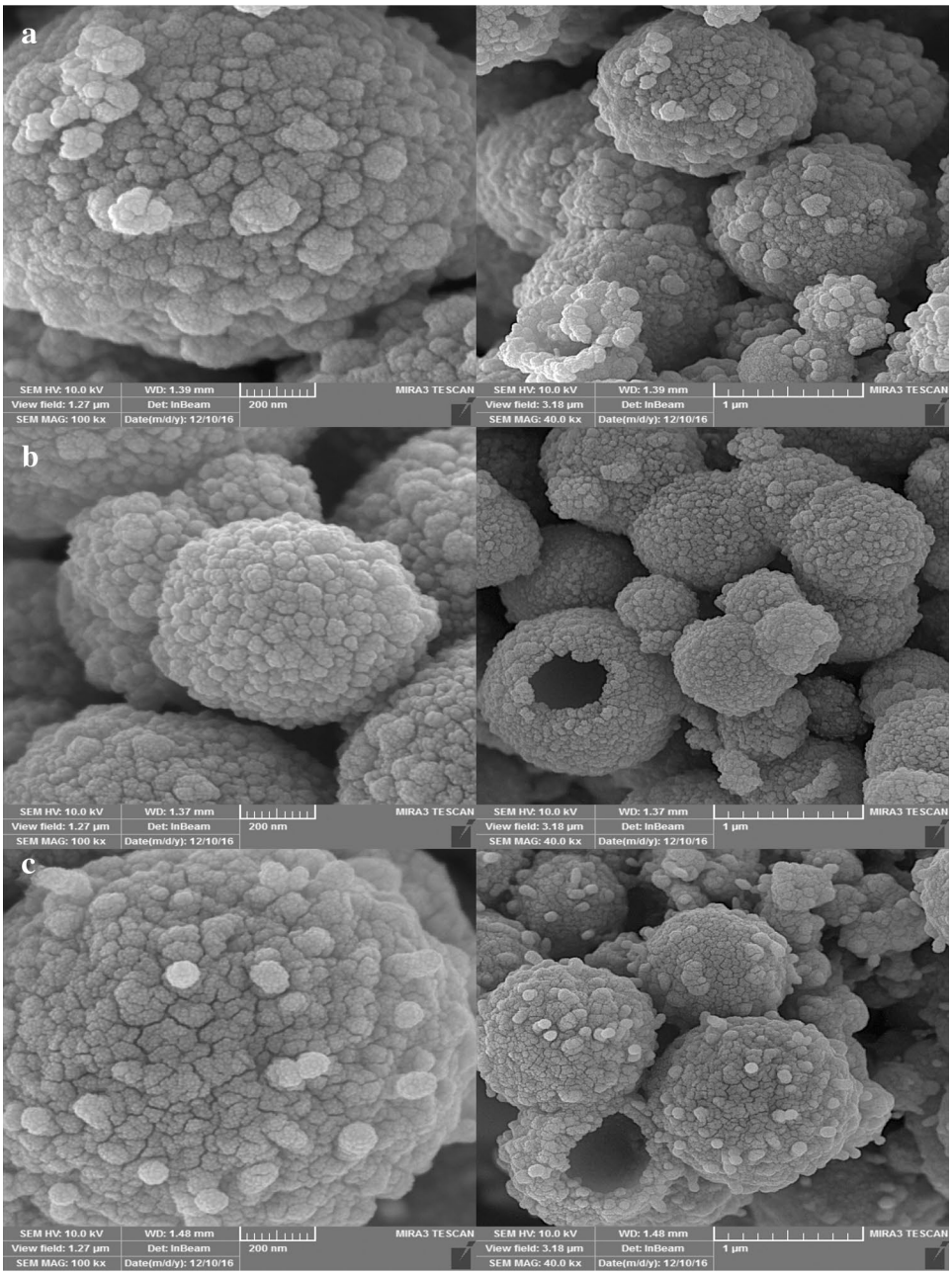

Fig. 5 SEM images of CuO/ZnO nanocomposites at **a** 5 min, **b** 10 min, **c** 15 min

β is the width of the observed diffraction peak at its half maximum intensity (FWHM), K is the shape factor, which takes a value of about 0.9, and λ is the X-ray wavelength (CuKα radiation, equals to 0.154 nm) were about 19.4 nm for CuO/ZnO nanocomposite. EDS analysis was applied for better investigation purity of CuO/ZnO nanocomposites. Figure 2 confirms that CuO/ZnO nanocomposite have prepared at high purity with any impurity.

Figure 3 shows FT-IR spectroscopy of CuO/ZnO nanocomposites. The absorption peak at 3444.48 cm^{-1} related to the stretching vibrational absorptions of OH. Double absorption peaks at 436.50 cm^{-1} corresponded to the stretching vibration of Zn–O and Cu–O.

For investigation morphology of nanocomposite scanning electron microscopy (SEM) was applied. Morphology and size of nanocomposite play important role on photocatalytic activity. So the synthesis procedure is done at various condition for obtaining optimum condition. For synthesis of CuO/ZnO nanocomposite, both modes of continuous and cyclic was applied. One cycle is 1 min long and composes of irradiation and non-irradiation for 30 s each. As well as shown in Fig. 4, the size of hollow spheres at continuous mode is less than the cyclic mode. In cyclic mode, growth of spheres overcomes to nucleation at power off period. This can lead to aggregation of particles and increase diameter of spheres.

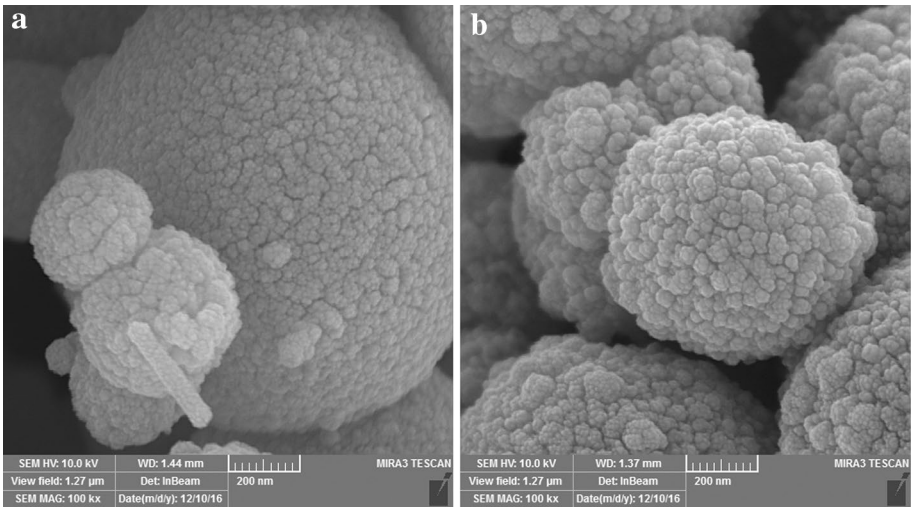

Fig. 6 SEM images of CuO/ZnO nanocomposites at **a** 750 W, **b** 900 W microwave irradiation

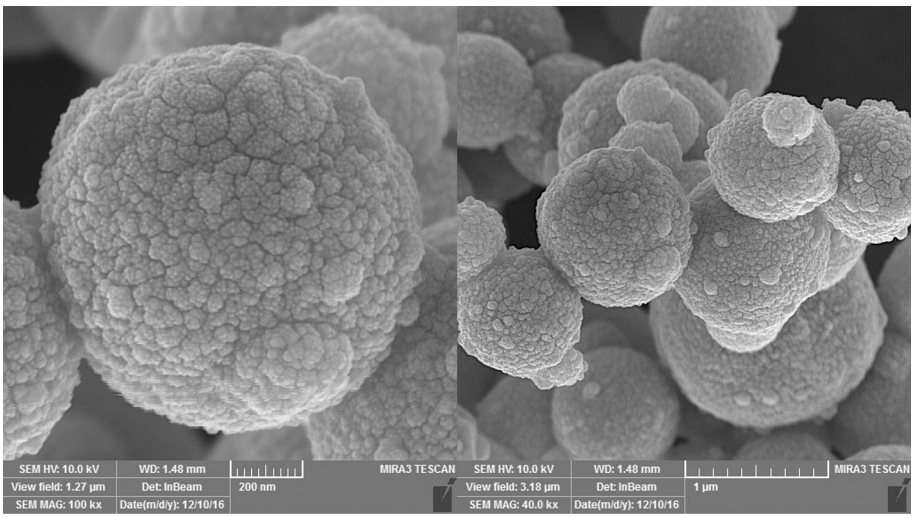

Fig. 7 SEM images of CuO/ZnO nanocomposites at 10 ml solvent volume

Figure 5 shows effect of irradiation time on morphology and size of CuO/ZnO nanocomposite. Before 5 min, no precipitation is formed. After 5 min irradiation, nanocomposite start to forming, but for the tiny size of formed sphere, aggregation occurs. Figure 5b reveals at 10 min spheres are smaller and homogenous. At time 15 min, small length nanorods start to form on the surface of spheres (Fig. 5c).

Figure 6 shows effect of microwave power on morphology and size of spheres at 10 min. At the powers smaller than 600 W, no product is formed. At the 750 W, spheres are not uniform, but at the 900 W, prepared spheres are uniform and homogenous.

Figure 7 shows effect of solvent volume on size of hollow sphere. Ethylene glycol play dual role in synthesis procedure: solvent and capping agent. When volume of ethylene glycol increases, the size of spheres decrease, so aggregation process occurs.

Effect of precursor on morphology and size of spheres is shown in Fig. 8. When $Zn(sal)_2$ and $Cu(sal)_2$ used instead of $Cu(CH_3CO_2)_2{\cdot}4H_2O$ and $Zn(CH_3CO_2)_2{\cdot}2H_2O$ respectively, since the enhance of steric hindrance, size of spheres decreases and subsequently aggregation process occurs.

Figure 8 illustrates diffuse reflectance spectra (DRS) of prepared CuO/ZnO nanocomposite. It shows optical absorption capability in the region from 200 to 800 nm. The optical energy band gap of nanocomposite was determined using the relation: $(\alpha h\vartheta) = C\ (h\vartheta - Eg)^{1/2}$. For this nanocomposite two band gap determined: 2.96 and 4 eV for CuO and ZnO respectively. These optical properties imply that CuO/ZnO nanocomposites can be applied as a good catalyst under UV light in photocatalyst process.

Figure 9 shows photocatalytic activity of prepared CuO/ZnO nanocomposites for RB and MB solutions after 120 min. As well as shown, 41 and 73% of RB and MB

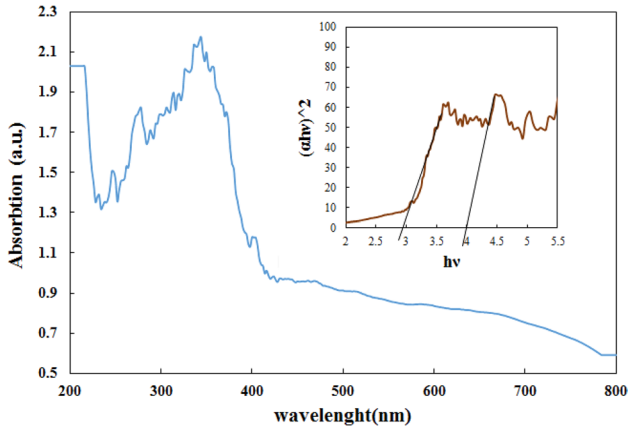

Fig. 8 DRS analysis of prepared CuO/ZnO nanocomposites. *Inset* calculated band gap for CuO/ZnO nanocomposites

was degraded respectively. The band position of CuO/ZnO system can lead to charge transfer from CuO to ZnO. So, recombination of electron–hole possibility in CuO becomes small and causes holes in valance band react with OH groups on the surface of nanocomposite and convert them to highly reactive OH· radicals. Produced radicals react with RB and MB and degraded.

4 Conclusion

In summary, hollow sphere of CuO/ZnO prepared via simple, fast and green microwave assisted method. For investigation and achievement to optimum conditions of synthesis procedure, X-ray diffraction (XRD) analysis, Fourier transform infrared (FT-IR) spectroscopy, scanning electron microscopy (SEM) and for an estimate the band gap used diffuse reflectance measurement (DRS) are applied. Optimum conditions for time, power and solvent volume are obtained 10 min, 900 W and 6 ml respectively. For the sustainable optical properties, prepared CuO/ZnO nanocomposites are applied as a catalyst in photodegradation of RB and MB pollutants. Results showed that after 120 min, 41 and 73% of RB and MB was degraded respectively.

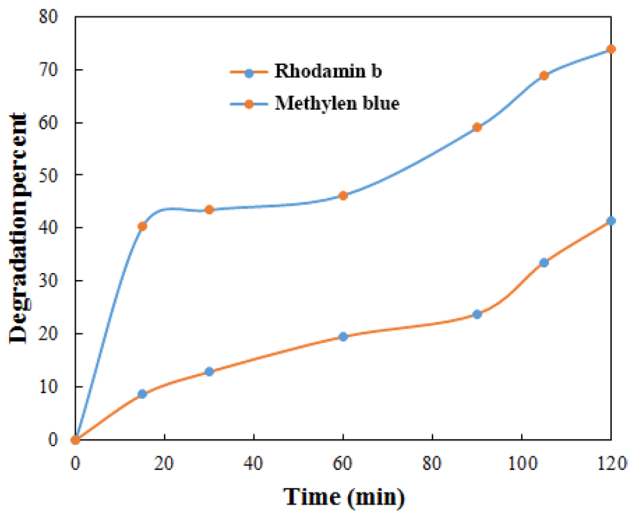

Fig. 9 Photocatalytic activity of CuO/ZnO nanocomposites under UV light

Acknowledgements Authors are grateful to the council of Iran National Science Foundation (INSF) and University of Kashan for supporting this work by Grant No (159271/8079).

References

1. M. El-Kemary, H. El-Shamy, I. El-Mehasseb, Photocatalytic degradation of ciprofloxacin drug in water using ZnO nanoparticles. J. Lumin. **130**, 2327–2331 (2010)
2. L. Xu, Y. Zhou, Z. Wu, G. Zheng, J. He, Y. Zhou, Improved photocatalytic activity of nanocrystalline ZnO by coupling with CuO. J. Phys. Chem. Solids **106**, 29–36 (2017)
3. Z. Zhu, X. Tang, C. Ma, M. Song, N. Gao, Y. Wang, P. Huo, Z. Lu, Y. Yan, Fabrication of conductive and high-dispersed Ppy@Ag/g-C_3N_4 composite photocatalysts for removing various pollutants in water. Appl. Surf. Sci. **387**, 366–374 (2016)
4. M. Hassanpour, H. Safardoust-Hojaghan, M. Salavati-Niasari, Degradation of methylene blue and Rhodamine B as water pollutants via green synthesized Co_3O_4/ZnO nanocomposite. J. Mol. Liq. **229**, 293–299 (2017)
5. R.L. Pérez, G.M. Escandar, Experimental and chemometric strategies for the development of green analytical chemistry (GAC) spectroscopic methods for the determination of organic pollutants in natural waters. Sustain. Chem. Pharm. **4** 1–12 (2016)
6. G. Eremektar, H. Selcuk, S. Meric, Investigation of the relation between COD fractions and the toxicity in a textile finishing industry wastewater: effect of preozonation. Desalination **211**, 314–320 (2007)
7. P. Moridi, F. Atabi, J. Nouri, R. Yarahmadi, Selection of optimized air pollutant filtration technologies for petrochemical industries through multiple-attribute decision-making. J. Environ. Manag. **197**, 456–463 (2017)
8. M.C. Pazos, M.A. Castro, A. Cota, F.J. Osuna, E. Pavón, M.D. Alba, New insights into surface-functionalized swelling high charged micas: their adsorption performance for non-ionic organic pollutants. J. Ind. Eng. Chem. (2017). doi:10.1016/j.jiec.2017.03.042
9. I. Ali, Z.A. Al-Othman, A. Alwarthan, Green synthesis of functionalized iron nano particles and molecular liquid phase adsorption of ametryn from water. J. Mol. Liq. **221**, 1168–1174 (2016)
10. A.M.E. Khalil, O. Eljamal, T.W.M. Amen, Y. Sugihara, N. Matsunaga, Optimized nano-scale zero-valent iron supported on treated activated carbon for enhanced nitrate and phosphate removal from water. Chem. Eng. J. **309**, 349–365 (2017)
11. A.M. Atta, H.A. Al-Lohedan, A.O. Ezzat, A.M. Tawfik, A.I. Hashem, Synthesis of zinc oxide nanocomposites using poly (ionic liquids) based on quaternary ammonium acrylamidomethyl propane sulfonate for water treatment. J. Mol. Liq. **236**, 38–47 (2017)
12. I. Ali, Z.A. Al-Othman, A. Alwarthan, Synthesis of composite iron nano adsorbent and removal of ibuprofen drug residue from water. J. Mol. Liq. **219**, 858–864 (2016)

13. H. Safardoust-Hojaghan, M. Salavati-Niasari, Degradation of methylene blue as a pollutant with N-doped graphene quantum dot/titanium dioxide nanocomposite. J. Clean. Prod. **148**, 31–36 (2017)
14. W. Shi, F. Guo, S. Yuan, In situ synthesis of Z-scheme Ag_3PO_4/$CuBi_2O_4$ photocatalysts and enhanced photocatalytic performance for the degradation of tetracycline under visible light irradiation. Appl. Catal. B **209**, 720–728 (2017)
15. J. Tu, X. Zeng, F. Xu, X. Wu, Y. Tian, X. Hou, Z. Long, Microwave-induced fast incorporation of titanium into UiO-66 metal-organic frameworks for enhanced photocatalytic properties. Chem. Commun. **53**, 3361–3364 (2017)
16. K. Gandha, J. Mohapatra, M.K. Hossain, K. Elkins, N. Poudyal, K. Rajeshwar, J.P. Liu, Mesoporous iron oxide nanowires: synthesis, magnetic and photocatalytic properties. RSC Adv. **6**, 90537–90546 (2016)
17. C. Karunakaran, P. Vinayagamoorthy, Superparamagnetic core/shell Fe_2O_3/ZnO nanosheets as photocatalyst cum bactericide. Catal. Today **284**, 114–120 (2017)
18. S.I. Al-Mayman, M.S. Al-Johani, M.M. Mohamed, Y.S. Al-Zeghayer, S.M. Ramay, A.S. Al-Awadi, M.A. Soliman, TiO_2ZnO photocatalysts synthesized by sol–gel auto-ignition technique for hydrogen production. Int. J. Hydrog. Energy **42**, 5016–5025 (2017)
19. L. Renuka, K.S. Anantharaju, Y.S. Vidya, H.P. Nagaswarupa, S.C. Prashantha, S.C. Sharma, H. Nagabhushana, G.P. Darshan, A simple combustion method for the synthesis of multi-functional ZrO_2/CuO nanocomposites: excellent performance as Sunlight photocatalysts and enhanced latent fingerprint detection. Appl. Catal. B **210**, 97–115 (2017)
20. K.-T. Lee, K.-P. Wai, S.-Y. Lu, CuO nanorods from carrier solvent assisted interfacial reaction processes: an unexpected extraordinary Fe-free photocatalyst in sunlight assisted Fenton-like processes. J. Taiwan Inst. Chem. Eng. **70**, 244–251 (2017)
21. P. Senthil Kumar, M. Selvakumar, S. Ganesh Babu, S. Induja, S. Karuthapandian, CuO/ZnO nanorods: an affordable efficient p-n heterojunction and morphology dependent photocatalytic activity against organic contaminants. J. Alloys Compd. **701**, 562–573 (2017)
22. R.R. Prabhu, A.C. Saritha, M.R. Shijeesh, M.K. Jayaraj, Fabrication of p-CuO/n-ZnO heterojunction diode via sol-gel spin coating technique, Mater. Sci. Eng. B **220** 82–90 (2017)
23. P. Lu, W. Zhou, Y. Li, J. Wang, P. Wu, Abnormal room temperature ferromagnetism in CuO/ZnO nanocomposites via hydrothermal method. Appl. Surf. Sci. **399**, 396–402 (2017)
24. M. Hassanpour, H. Safardoust, D. Ghanbari, M. Salavati-Niasari, Microwave synthesis of CuO/NiO magnetic nanocomposites and its application in photo-degradation of methyl orange. J. Mater. Sci. Mater. Electron. **27**, 2718–2727 (2016)